Journal of Applied Polymer Science

# Uniaxial Tensile Properties of $TiO_2$ Coated Single Wool Fibers by Sol-Gel Method: The Effect of Heat Treatment

**Baki Aksakal,[1] Kenan Koc,[1] Altan Bozdogan,[1] Katherina Tsobkallo[2]**

[1]Department of Physics, Davutpasa Campus, Yildiz Technical University, Esenler 34210, Istanbul, Turkey

[2]Department of Mechanics of Materials, St. Petersburg State University of Technology and Design, B. Morskaya 18, 191186, St. Petersburg, Russia

Correspondence to: B. Aksakal (E-mail: aksakal@yildiz.edu.tr)

**ABSTRACT:** Single wool fibers were coated with $TiO_2$ by using the sol-gel method. The uniaxial tensile properties of $TiO_2$ coated single wool fibers heated at different temperatures from 25 to 200°C were investigated and compared with those of uncoated single wool fibers. It was observed that the shape of the stress–strain curve of $TiO_2$ coated wool fibers became the same as uncoated wool fibers and showed a similar tendency of change to uncoated wool fibers with increasing temperature. But, the $TiO_2$ coated wool fibers obtained higher rigidity than uncoated wool fibers and up to their rupture points; they obtained higher stress levels in three deformation regions in the stress–strain curves, which indicates stronger wool fibers. Although the breaking extension of $TiO_2$ coated wool fibers decreased little by about 8%, the Young's modulus of $TiO_2$ coated wool fibers increased significantly by 19%, which was caused mostly by an increment in the stiffness of the cuticle layer of the wool fiber, and remained relatively higher than that of uncoated wool fibers after heat treatments. Structural changes in both uncoated and $TiO_2$ coated single wool fibers due to thermal effect, which caused the changes in the uniaxial tensile properties and the thermal behaviors of these fibers were discussed by using spectroscopic and thermal analysis methods in detail. © 2013 Wiley Periodicals, Inc. J. Appl. Polym. Sci. 130: 898–907, 2013

**KEYWORDS:** mechanical properties; thermal properties; fibers

Received 11 December 2012; accepted 15 February 2013; published online 11 April 2013
**DOI: 10.1002/app.39162**

## INTRODUCTION

Wool fibers mostly used for the production of different textile materials in wool industry have a complex structure consisting of two main morphological components. The first component considered as mechanically the most important component is a cortex having mainly amorphous matrix phase consisting of matrix globules and microfibrils representing crystalline part that are composed of mainly α-helical structures.[1–3] Matrix globules are connected with each other and with microfibrils by disulfide crosslinks and different kinds of intermolecular interactions.[1] The α-helices in microfibrils are generally held together by intra- and intermolecular interactions such as hydrogen bonds, disulfide bonds (crosslinks) between two cysteine residues,[3,4] a salt bridge between an arginine residue, and a glutamic acid residue.[5] The second component is the cuticle layer consisting of cuticle cells or scales being richer in β-sheet and/or disordered regions[6,7] and it was shown that the cuticle structure is noncrystalline and amorphous protein.[8,9] It was also shown on the basis of three-component model[10] that the contribution of the cuticle to the stiffness of a wool fiber is significant and about 20%. It is known that both cuticle cells and cortex region consist of similar amino acid residues such as glycine, alanine, and cysteine with different proportions.[6,7,11] Considering the proportions of the amino acids, cysteine, proline, serine, and valine residues, which are generally thought to be nonhelical forming amino acid residues are found in the cuticle cells at higher proportions than in cortical cells.[6] On the other hand, cuticle cells have lower content of some amino acids such as glutamic acid, phenylalanine, threonine, arginine, leucine, and aspartic acid.[6]

Considering the applications of wool fibers in textile industry, it is known that there are some serious problems such as photo yellowing and aging of wool under UV radiation. In recent years, in order to improve the photostability of wool fabrics and some other properties, some inorganic particles such as Titanium dioxide ($TiO_2$) nanoparticles being cheap, nontoxic, and photostable have been used as inorganic UV blockers.[12–15] Besides, $TiO_2$ nanoparticles have been used to improve antifelting and antibacterial properties,[16] self-cleaning property,[13,17] as well as some other properties of woolen fabrics.[18] However,

how the uniaxial tensile properties of single wool fibers change after coated with $TiO_2$ by sol-gel method was not investigated in detail except few studies on wool fabrics.[13,19]

It is known that the properties of wool fibers change after they are exposed to thermal effect. Many studies were devoted to understand the thermal characteristics of the wool fibers on the basis of structural changes[20–22] and the effect of temperature on the spectroscopic properties, the stress–strain curves, and the tensile properties of wool fibers.[3,11,23–25] However, the tensile characteristics of the wool fibers after the wool fibers were exposed to heat treatment at different elevated temperatures were not investigated much in detail. Although it is known that $TiO_2$ improves the some properties of wool fibers such as photostability, antibacterial, and antifelting properties, it is not investigated how the uniaxial tensile properties of the single wool fibers coated by sol-gel method change after exposed to heat treatment. Thus, our study aimed to investigate mainly the uniaxial tensile properties of $TiO_2$ coated wool fibers by sol-gel method and their changes after heat treatment at various temperatures from 25 to 200°C and compare these changes with those of uncoated wool fibers. Therefore, the responsible structural changes for the changes in the stress–strain curve and uniaxial tensile properties of uncoated and $TiO_2$ coated wool fibers were discussed by using tensile testing, spectroscopic, and thermogravimetric methods.

## EXPERIMENTAL

### Materials

**Preparation of $TiO_2$ Sol and $TiO_2$ Coated Wool Fibers.** In this study, white wool fibers originating from Turkey were used. To obtain $TiO_2$ coated wool fibers by sol-gel method, $TiO_2$ sol was prepared as described earlier[26] in two steps using titanium (IV) butoxide ($Ti[O(CH_2)_3CH_3]_4$, TIVBT) [>97% Sigma-Aldrich, Inc. USA]. In the first step, TIVBT, ethanol (EtOH) [99.8% Riedel-deHaën, Germany] and acetic acid ($CH_3COOH$) [100% Merck, Germany] were mixed at room temperature for 30 min under the molar ratios TIVBT : EtOH : $CH_3COOH$ = 1 : 113.45 : 1.4. In the second step, ethanol was added to the solution so that the molar ratios became TIVBT : EtOH : $CH_3COOH$ = 1 : 189.1 : 1.4. After this, the solution was stirred for 1 h more at room temperature. $TiO_2$ solutions came out homogeneous and transparent. Single wool fibers were kept in $TiO_2$ sol for ~1 min and then were dried at room conditions ($T$ = 25°C, RH = 60%) for 1 h. Later, the wool samples were kept at 105°C for 5 min to remove volatile species.

### Methods

**Tensile Testing.** Uniaxial tensile tests of uncoated and $TiO_2$ coated single wool fibers having an average diameter of 73 ± 3 $\mu$m and a gauge length of 5 cm were made on a Lloyd tensile testing machine LF *Plus* (AMETEK Lloyd Inst., UK) with a crosshead speed of 50 mm/min at room conditions ($T$ = 25°C; RH = 60%). For the thermal treatment, the samples were heated at different temperatures ranging from 25 to 200°C for 30 min. Then, the tensile tests of the heated single wool fibers were carried out at the same conditions.

**Scanning Electron Microscopy (SEM).** SEM measurements of both uncoated and $TiO_2$ coated wool fibers were carried out on a JEOL JMS 5410 LV microscope (Japan) with an applied voltage of 20.0 kV and magnification of 500.

**X-Ray Flourescence (XRF) Spectroscopy.** Before the XRF spectroscopy measurements, several single wool fibers were placed parallel very close to each other in order to remove the spaces among themselves and stuck in a small rectangular frame. Later, the XRF measurements of the uncoated and $TiO_2$ coated wool fibers were done on a Midex M XRF spectrometer (Spectro, Germany).

**Thermogravimetric Analysis (TGA).** TGA and differential scanning calorimetry (DSC) measurements were performed on about 3 mg of the uncoated and $TiO_2$ coated wool fibers by using a SDT Q600 thermogravimetric analyzer (TA Instruments, USA) under a nitrogen atmosphere with a heating rate of 10°C/min over the range of 30–600°C.

**Spectroscopic Measurements.** The infrared experiments were carried out on a Fourier transform spectrometer "Spectrum One" (PerkinElmer, Inc. USA) utilizing the ATR (Attenuated Total Reflectance) cell. The FTIR/ATR spectrum of uncoated and $TiO_2$ coated wool fibers heated from 25 to 250°C were obtained at room conditions. For each measurement, 14 single wool fibers placed very close and parallel to each other in a rectangular frame were used. FTIR/ATR spectra of the samples were recorded in the 550–4000 $cm^{-1}$ range at a resolution of 4 $cm^{-1}$ with 4 scans for each measurement. For obtaining the FTIR/ATR spectrum of $TiO_2$ powder, a sufficient amount of $TiO_2$ powder (~1 mg) obtained from $TiO_2$ sol was clamped against the vertical face of the ATR crystal and then the spectrum was recorded.

## RESULTS AND DISCUSSION

### XRF and SEM Results of Uncoated and $TiO_2$ Coated Wool Fibers

XRF spectra of $TiO_2$ coated and uncoated wool fibers were recorded from different points and samples and very similar XRF spectra and results were obtained, which indicated that the wool fibers were coated with $TiO_2$ uniformly. As a comparison, one of these XRF spectra of uncoated and $TiO_2$ coated wool fibers is given in Figure 1. Here, $TiO_2$ coated wool fibers showed two prominent peaks of high intensity due to the $K_{\alpha 1}$ and $K_{\beta 1}$ transitions in Titanium, which evidence that wool fibers were coated with $TiO_2$ network. Besides, in order to see how $TiO_2$ coating affects the surface of the wool fibers, the SEM images of $TiO_2$ coated wool fiber and uncoated wool fiber were obtained and are shown in Figure 2 as a comparison. Here, it is seen the cuticle layer of the wool fiber was affected significantly by coating with $TiO_2$. As seen in Figure 2(b), $TiO_2$ coated wool fiber shows that the cuticle layer of the wool fiber was covered with a $TiO_2$ sol and $TiO_2$ sol filled in each cuticle cell uniformly. Thus, on the molecular level, a $TiO_2$ network was formed on the cuticle layer, the formation mechanism of which will be discussed in subsequent parts.

### Uniaxial Tensile Properties

Uniaxial tensile characteristics such as initial or Young's modulus ($E_i$), breaking extension ($\varepsilon_b$), ultimate tensile stress ($\sigma_u$), and the work of rupture ($U$) of a wool fiber are obtained from the

Applied Polymer SCIENCE

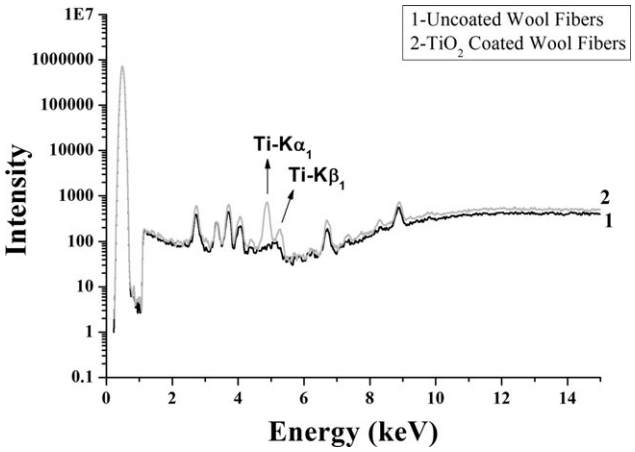


**Figure 1.** XRF spectrum of the wool fibers.

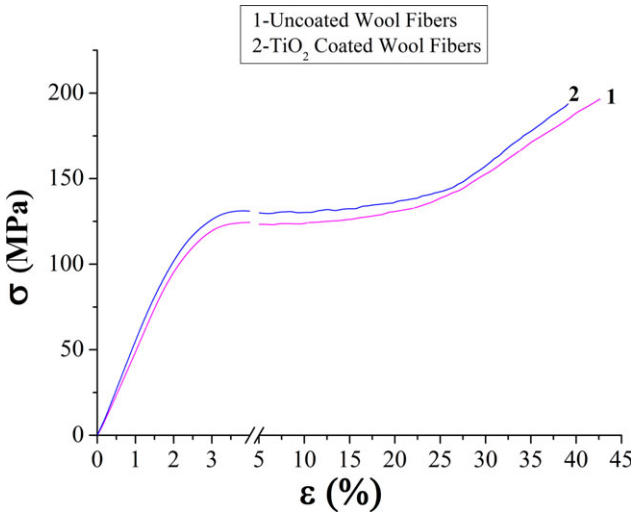


**Figure 3.** The representative stress–strain curves of the wool fibers at 25°C. [Color figure can be viewed in the online issue, which is available at wileyonlinelibrary.com.]

well-known stress–strain diagram commonly divided into three regions: an initial linear region generally referred to as a Hookean region from 0 to 2%, the yield region extending from 2 to 25–30% strain, and the post yield region beyond about 30% strain.[3,27–30] It is seen from the comparison of the stress–strain curves of uncoated and $TiO_2$ coated wool fibers at room conditions ($T = 25°C$; RH = 60%) shown in Figure 3, that the shape of the stress–strain curve of $TiO_2$ coated wool fiber did not become different from that of uncoated wool fiber and the stress–strain curve $TiO_2$ coated wool fibers showed three deformation regions commonly. Here, it is seen that the stiffness or rigidity increased, hence, from the tensile properties, especially the initial modulus increased significantly by around 19% as seen from the comparison of the values in Tables I and II. Because of increasing rigidity, although the breaking extension slightly decreased by about 8%, the ultimate tensile stress became almost the same as that of uncoated wool fibers and changed only by 1%. The work of rupture also decreased little by about 3%. Although the yield strain ($\varepsilon_y$) almost did not change at all, the yield stress ($\sigma_y$) got higher stress value indicating more rigid fiber.

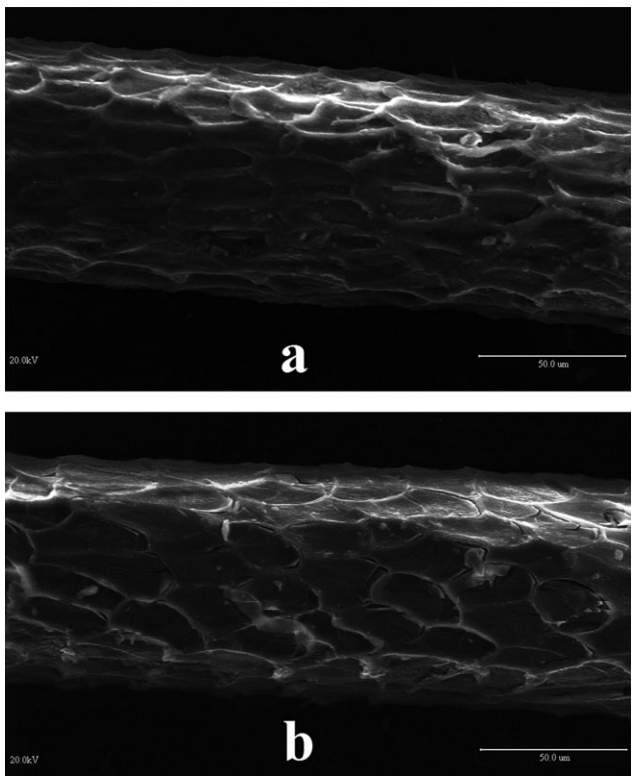


**Figure 2.** SEM images of (a) uncoated and (b) $TiO_2$ coated wool fibers.

When uncoated and $TiO_2$ coated wool fibers were heated at $T = 75°C$, it was seen that the stress–strain curve of $TiO_2$ coated wool is similar to that of uncoated wool fiber as shown in Figure 4 and $TiO_2$ coated wool fibers obtained higher stress values in the linear, yield and post yield regions than those of uncoated wool fibers. This shows that $TiO_2$ coated wool fibers obtained stronger and more rigid structure than that of uncoated wool fiber up to their breakage. Besides, the initial modulus almost did not change when compared with that at room condition but remained higher than that of corresponding uncoated fiber.

Moreover, when the fibers were heated at 150 and 175°C, it was seen on the stress-strain curves shown in Figures 5 and 6 that the $\sigma_u$ and $\varepsilon_b$ values of $TiO_2$ coated wool fibers did not decrease significantly. They became close to those of uncoated wool fibers. However, corresponding initial modulus values with a decreasing tendency remained higher than those of uncoated wool fibers. Here, the prominent changes were seen in the slope of the yield region for both uncoated and $TiO_2$ coated wool fibers as shown in Figures 5 and 6. They became higher than their corresponding values for wool fibers at room conditions.

After the fibers were heated at $T = 200°C$, remarkable changes were seen in both stress–strain curves and the tensile characteristics as seen in Figure 7 and Tables I and II. Both samples did not have a post yield region, which shows that the fiber broke down before the $\alpha$–$\beta$ conformational transitions did not complete fully. Breaking extension and the work of rupture values

**Table I.** Mean and Standard Deviation Values of Uniaxial Tensile Properties of Uncoated Wool Fibers after Being Heated at Different Temperatures for 30 min

| $T$ (°C) | $E_i$ (GPa) | $\varepsilon_y$ (%) | $\sigma_y$ (MPa) | $\varepsilon_b$ (%) | $\sigma_u$ (MPa) | $U$ (mJ) |
|---|---|---|---|---|---|---|
| 25 | 5.13 ± 0.4 | 3.6 ± 0.1 | 125 ± 5 | 42.6 ± 2.1 | 196 ± 7 | 14.0 ± 1.0 |
| 75 | 5.16 ± 0.4 | 4.0 ± 0.1 | 130 ± 5 | 41.2 ± 1.6 | 195 ± 6 | 13.5 ± 0.7 |
| 150 | 5.15 ± 0.5 | 4.1 ± 0.2 | 117 ± 6 | 38.9 ± 2.4 | 191 ± 10 | 12.1 ± 1.0 |
| 175 | 5.02 ± 0.6 | 3.6 ± 0.2 | 110 ± 4 | 37.1 ± 3.5 | 180 ± 6 | 10.4 ± 0.8 |
| 200 | 4.97 ± 0.1 | 5.6 ± 1.0 | 126 ± 1 | 22.1 ± 5.1 | 144 ± 5 | 4.7 ± 1.2 |

decreased dramatically, that is, by 48% and 66% for uncoated wool fibers and 64% and 77% for $TiO_2$ coated wool fibers with respect to those at room conditions. This shows that the fibers became much weaker and lost the most of the mechanical properties, especially the extensibility. Heating at higher temperatures than 200°C made both uncoated and $TiO_2$ coated wool fibers very brittle and changed their colors from white to brown, thus the uniaxial tensile tests could not be carried out.

### Thermal Analysis

The TGA and DSC curves of uncoated and $TiO_2$ coated wool fibers are shown in Figure 8. The mass loss and enthalpy values of the endothermic peaks seen in DSC curves for uncoated and $TiO_2$ coated wool fibers are given in Tables III and IV. From the comparison, it is clearly seen that TGA curves of both samples are very close to each other and show a similar characteristic. Here the TGA curves can be divided approximately into three regions. The first region up to about 160°C is attributed to the vaporization of the absorbed water and dehydration of wool,[25,31–33] which is characterized by an initial broad endothermic peak at about 92°C. Here, the mass loss of $TiO_2$ coated wool fiber is more than that of uncoated wool fibers because of appearance of water molecules during the formation of $TiO_2$ network on the cuticle layer. The second region between about 210 and 360°C, in which the mass losses of $TiO_2$ coated and uncoated wool fibers are almost the same, corresponds to the denaturation and degradation of wool fiber structure.[25,33,34] Here, there are some similar explanations for this denaturation and degradation process. For example, this wide endothermic peak is attributed to the hydrogen-bond peptide helical structure ruptures and that the ordered regions of the wool undergo a solid to liquid phase change as well as cleavage of the disulfide bonds releasing a number of volatiles including hydrogen sulfide and sulfur dioxide.[34] According to Menefee and Yee[35] the melting of the major ordered part of the wool protein occurs at 235°C, disulfide bond cleavage takes place at around 230–250°C, and general pyrolysis happens above 250°C. Manich et al.[36] observed two denaturation peaks at around 210 and 230°C associated with the denaturation of ortho-cortical and the para-cortical cells of the fiber and stated that the thermal degradation of keratin and other histological components of the wool dried fiber takes place at temperatures exceeding 232°C.

Thus we assume that the endothermic peak observed at about 242 and 241°C with enthalpy values of 1.5 and 1.2 J/g for uncoated and $TiO_2$ coated wool fibers, respectively can be attributed to the α-keratin denaturation and it is probably related to the denaturation of para-cortical cells. Following broad endothermic peak observed from about 250 to 360°C with enthalpy values of 146.9 and 110.4 J/g for uncoated and $TiO_2$ coated wool fibers, respectively, can be attributed to the degradation of α-keratin and other histological components, that is, the rupture of α-helical structures, cleavages of disulfide bonds, and the degradation of the matrix structure. Here, it is seen that the required enthalpy and the roughly estimated peak temperature for the degradation process in $TiO_2$ coated wool fiber is less than that in uncoated wool fiber. This implies the $TiO_2$ sol catalyzes the thermal decomposition of the wool fiber.[33] In the third region beyond 360°C, an exothermic reaction, i.e., the char oxidation reaction takes place in the wool.[33] Here, the mass loss of the $TiO_2$ coated wool fiber became about 22% being slightly less than that of uncoated wool fibers.

### FTIR/ATR Spectral Analysis

The FTIR/ATR spectra of $TiO_2$ powder obtained from $TiO_2$ sol, uncoated, and $TiO_2$ coated wool fibers at room conditions are given in Figure 9. Here, in the spectrum of $TiO_2$ powder obtained from $TiO_2$ sol, the peak at about 800 $cm^{-1}$ is assigned to Ti—O stretching vibrations.[37,38] The bands in the regions of 1032, 1423, and 1532 $cm^{-1}$ are attributed to stretching and vibrations of the Ti—O—Ti group,[37] which indicate the

**Table II.** Mean and Standard Deviation Values of Uniaxial Tensile Properties of $TiO_2$ Coated Wool Fibers after Being Heated at Different Temperatures for 30 min

| $T$ (°C) | $E_i$ (GPa) | $\varepsilon_y$ (%) | $\sigma_y$ (MPa) | $\varepsilon_b$ (%) | $\sigma_u$ (MPa) | $U$ (mJ) |
|---|---|---|---|---|---|---|
| 25 | 6.13 ± 0.5 | 3.6 ± 0.1 | 138 ± 6 | 39.1 ± 1.2 | 194 ± 9 | 13.6 ± 0.5 |
| 75 | 5.98 ± 0.3 | 4.1 ± 0.2 | 137 ± 3 | 38.1 ± 1.7 | 192 ± 8 | 13.0 ± 0.9 |
| 150 | 5.97 ± 0.7 | 4.0 ± 0.2 | 119 ± 6 | 36.8 ± 3.1 | 189 ± 17 | 11.6 ± 1.4 |
| 175 | 5.37 ± 0.6 | 3.4 ± 0.1 | 115 ± 2 | 36.6 ± 1.2 | 179 ± 6 | 10.5 ± 0.9 |
| 200 | 5.23 ± 0.2 | 4.9 ± 0.5 | 126 ± 2 | 14.1 ± 5.0 | 140 ± 4 | 3.1 ± 0.8 |

Applied Polymer SCIENCE

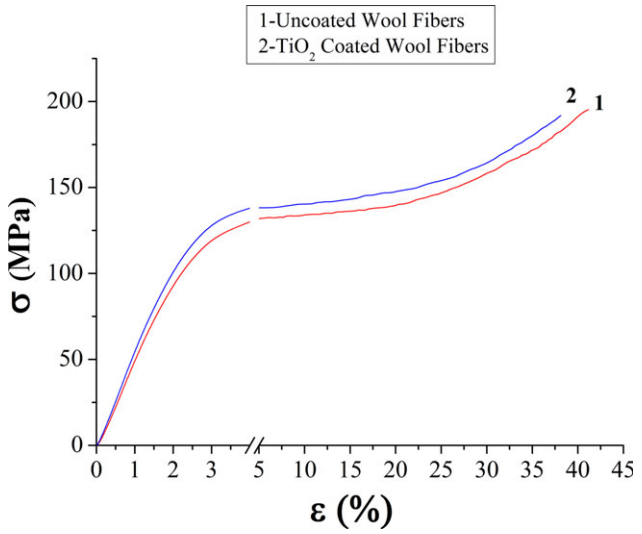


**Figure 4.** The representative stress–strain curves of the wool fibers after being heated at 75°C. [Color figure can be viewed in the online issue, which is available at wileyonlinelibrary.com.]

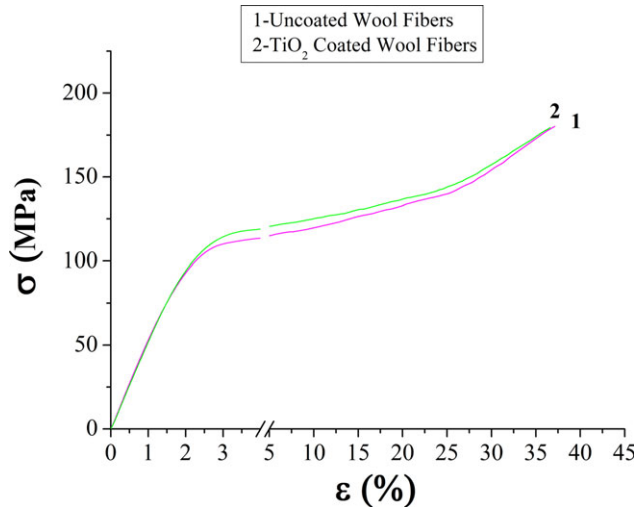


**Figure 6.** The representative stress–strain curves of the wool fibers after being heated at 175°C. [Color figure can be viewed in the online issue, which is available at wileyonlinelibrary.com.]

formation of the inorganic matrix. Another band, at 1128 $cm^{-1}$ is attributed to the Ti—O—C vibration due to Ti-butoxy species.[39] The peak observed at about 1248 $cm^{-1}$ is due to the C—H flexion (symmetric) of ethyl groups.[38] Another band, observed at 1711 $cm^{-1}$ with low intensity, is attributed to the C=O stretching of H-bonded acid groups.[40] The peaks at about 2856 and 2923 $cm^{-1}$ were attributed to the symmetric and asymmetric C—H stretching of $CH_2$,[41] respectively. A broad OH band centered at about 3180 $cm^{-1}$ is from occluded $H_2O$, ethanol, and OH from the hydroxy (Ti—OH) groups.[38]

In the spectrum of uncoated wool fibers as seen in Figure 9, well known the Amide I, II, and III bands[4,31,42–44] are observed at about 1630, 1518, and 1234 $cm^{-1}$. Another band observed at about 1452 $cm^{-1}$ is assigned to $CH_2$ bending mode.[4,42–44] The studies using infrared analysis of oxidized wool[45,46] and oxidized human hair[47–49] assigned the peaks at 1040 $cm^{-1}$ and l175 to 1180 $cm^{-1}$ to sulfonate linkages or sulfonic acid groups of cysteic acid residues. In the study[49] of infrared spectroscopy of oxidized hair, the band at 1188 $cm^{-1}$ was assigned to asymmetric sulfonate S=O stretching vibration, which was observed at around 1174 $cm^{-1}$ in our study.

Another peak observed at around 3070 $cm^{-1}$ was assigned to Amide B band,[50] which is connected with the frequency of stretching vibrations of located $\nu$(N—H) bonds.

The intensive band observed at around 3275 $cm^{-1}$ is attributed to the NH stretching of hydrogen-bonded NH groups (Amide A band).[30,31,41,50,51] Besides, another band observed at about

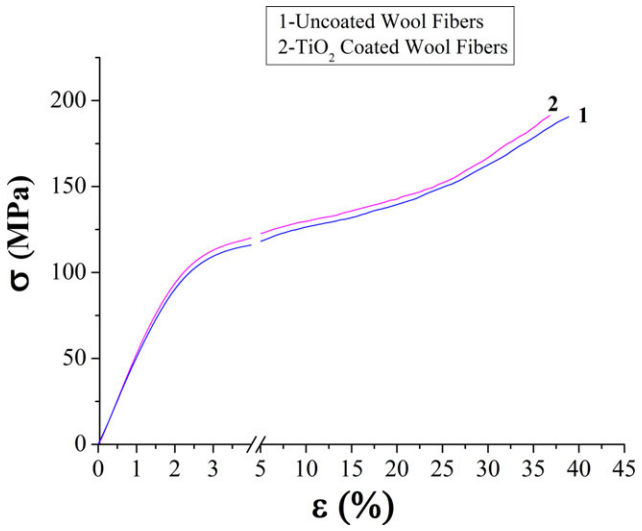


**Figure 5.** The representative stress–strain curves of the wool fibers after being heated at 150°C. [Color figure can be viewed in the online issue, which is available at wileyonlinelibrary.com.]

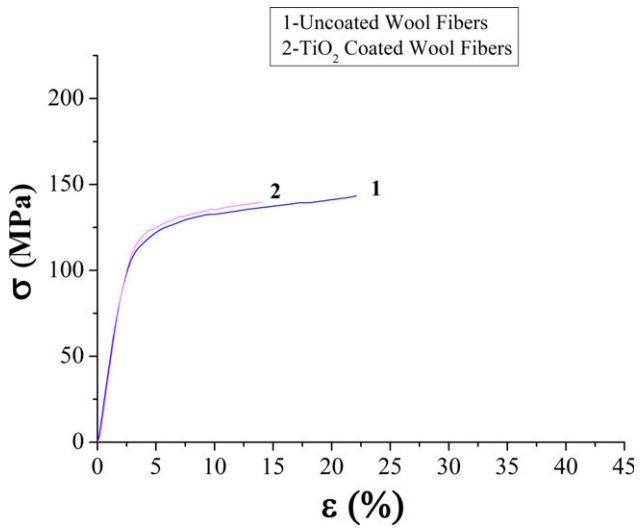


**Figure 7.** The representative stress–strain curves of the wool fibers after being heated at 200°C. [Color figure can be viewed in the online issue, which is available at wileyonlinelibrary.com.]

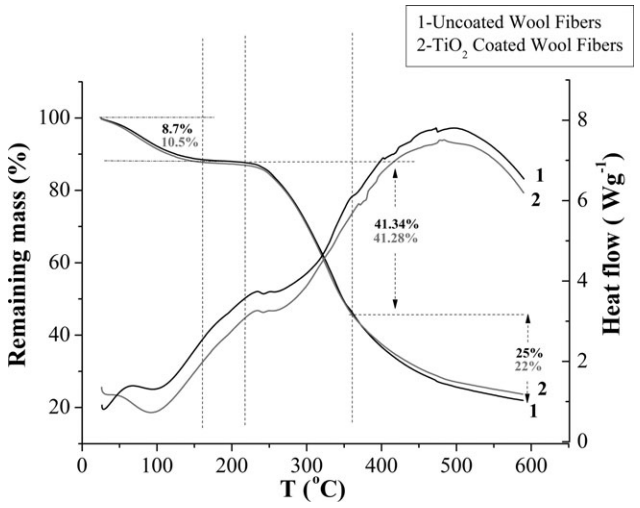


**Figure 8.** TGA/DSC curves of the wool fibers.

3400 $cm^{-1}$ is attributed to the vibration of the free NH groups.[30,51]

The bands observed at 2925 and 2853 $cm^{-1}$ are assigned to asymmetric and symmetric $CH_2$ stretch, respectively.[31,41,51,52] Similarly, the bands at 2957 and 2874 $cm^{-1}$ are attributed to asymmetric and symmetric $CH_3$ stretch, respectively.[51,52]

It is seen in Figure 9 that the spectra of $TiO_2$ coated wool fibers and uncoated wool fibers look too similar to each other. However, the $TiO_2$ coating led to two new bands at around 815 and 865 $cm^{-1}$ with low intensity belonging to Ti—O stretching vibrations, which were also seen in the spectrum of the $TiO_2$ powder. Because the absorbencies of Amide I, II, and III bands, which are the main characteristic bands of α-helical structure of the cortex region of the wool fiber did not change significantly in $TiO_2$ coated wool fiber, we think that the $TiO_2$ sol mostly interacted with the side chain molecules of the amino acids found in the cuticle cells of the cuticle layer rather than diffusing in to the cortex region. Besides, some increments were seen in the absorbencies of C—H stretching modes of $CH_3$ groups, because of existence of some residual molecules such as $CH_3$ of acetic acids and Titanium butoxide on the surface of wool fibers during the coating process. Moreover, our studies[30,53] revealed that the change in the hydrogen bond interactions in wool fibers examined by the analysis of the absorbencies of NH stretching vibrations and OH stretching of water molecules during deformation process significantly affects the mechanical properties of wool fibers. Thus, here it is clearly seen in Figure 9 that the absorbencies of the N—H stretching vibrations at around 3275 and 3400 $cm^{-1}$ increased significantly, because during coating process, $TiO_2$ network formed as a result of condensation and hydrolysis process and some free water molecules can be present in the cuticle cells, which can alter the absorbencies of free and hydrogen bonded N—H groups of the amino acids in the cuticle layer.

The changes of FTIR/ATR spectra of uncoated and $TiO_2$ coated wool fibers with increasing treatment temperatures are given in Figures 10 and 11, respectively. The absorbance ratios of the bands were calculated using an internal standard band, i.e., the $CH_2$ scissoring band at 1452 $cm^{-1}$.[4,42]

The changes in the absorbance ratio of the asymmetric C—H stretching mode of $CH_3$ with increasing temperature for both uncoated and $TiO_2$ coated samples are given in Figure 12. It is known from the structural compositions of the wool fibers that $CH_3$ molecules are present in the side chains of some amino acids such as serine, threonine, alanine in the cuticle layer and in the cortex region consisting of matrix and α-helical structures. In the case of $TiO_2$ coated wool fibers, in addition, some $CH_3$ molecules may be also present in the cuticle cells due to remaining residual groups from $TiO_2$ sol during the formation of $TiO_2$ network on the cuticle layer. Because of more $CH_3$ molecules in $TiO_2$ coated wool fibers, the absorbance ratio of this band became higher than that of uncoated wool fibers as shown in Figure 12. It is seen in Figure 12 that up to around 200°C, the absorbance ratios of asymmetric C—H stretching mode of $CH_3$ groups for both uncoated and $TiO_2$ coated wool fibers did not change much but decreased slightly caused by the deformation of these groups. However, after 200°C, the absorbance ratios decreased significantly due to the starting of great thermal degradation in the wool fibers, which caused the deformation or breakage of $CH_3$ groups.

Furthermore, spectral results revealed that also the disulfide bonds were affected by heat treatment. It is known that cystine residues link two polypeptide chains by disulfide crosslinks as interchain linkage or two components of the same polypeptide chain as an intrachain linkage. The presence of cystine in α-keratin fibers is primarily responsible for the high stability of the α-keratin fibers such as wool to the degradation caused by heat, cold, light, water, biological attack, and mechanical distortion.[3] We know that when the sulfur-sulfur bond of disulfide crosslinks is cleaved in oxidation reaction, sulfur containing residues such as sulfonic acids and sulfonate come out. This also leads to a significant increase in the amount of cysteic acid and a decrease in the amount of cystine in the wool fiber.

Figure 13 shows the change of the absorbance ratios of asymmetric S=O stretch of sulfonate groups for uncoated and $TiO_2$ coated wool fibers with increasing heat treatment temperature. We see that the changing tendency of the absorbance ratio of uncoated and $TiO_2$ coated wool fibers is the same. However, the absorbance of the asymmetric S=O stretch of sulfonate groups of cysteic acid residues in $TiO_2$ coated wool fibers is lower than

**Table III.** The Endothermic Peaks and Corresponding Enthalpy Values Observed in DSC Curves of Uncoated and $TiO_2$ Coated Wool Fibers

| | Water evaporation | | Denaturation + degradation | | | |
|---|---|---|---|---|---|---|
| | $T_w$ (°C) | $\Delta H_w$ (J/g) | $T_{den}$ (°C) | $\Delta H_{den}$ (J/g) | $T_{deg}$ (°C) | $\Delta H_{deg}$ (J/g) |
| Uncoated wool | 94 | 109.6 | 242 | 1.5 | 315 | 146.9 |
| $TiO_2$ coated wool | 92 | 182.1 | 241 | 1.2 | 300 | 110.4 |

**Table IV.** Mass Losses of Uncoated and $TiO_2$ Coated Wool Fibers

| | Water evaporation | | Denaturation + degradation | | Char oxidation | |
|---|---|---|---|---|---|---|
| | Temperature range (°C) | Mass loss (%) | Temperature range (°C) | Mass loss (%) | Temperature range (°C) | Mass loss (%) |
| Uncoated wool | 60-160 | 8.7 | 210-360 | 41.34 | 360-600 | 25 |
| $TiO_2$ coated wool | 45-160 | 10.5 | 210-360 | 41.28 | 360-600 | 22 |

that of uncoated wool fibers, because we suppose that present cysteic acid residues, which contain sulfonate (—$SO_3^-$) interacted with $TiO_2$ sol and some of them might be deformed or converted to different species, thus, they slightly reduced the absorbance of the sulfonate groups. Here, it is seen that up to around 200°C, for both uncoated and $TiO_2$ coated wool fibers, the absorbance ratio of the asymmetric sulfonate S=O stretching vibrations did not change and became almost stable, which can indicate almost no cleavage of disulfide crosslinks. However, after around 200°C, the absorbance ratio indicating the amount of sulfonate groups increased greatly. Thus, it proves the cleavages of disulfide bonds in both uncoated and $TiO_2$ coated wool fibers as a result of thermal destruction of the structure at high temperatures.

On the other hand, while $TiO_2$ network is formed on the surface of wool fibers, $TiO_2$ sol interacted with generally hydroxyl and carboxylic groups[13,54] of amino acid residues such as serine, threonine, tyrosine, aspartic, and glutamic acid and some water molecules can come out as a result of hydrolysis and condensation process. Therefore, these water molecules affect the amount of hydrogen bonded NH groups by forming hydrogen bonds with NH groups. The change of absorbance ratio of N—H stretching of hydrogen bonded NH groups in uncoated and $TiO_2$ coated wool fibers with increasing temperature is given in Figure 14. Here, it is seen that the absorbance ratio of NH stretching of hydrogen bonded NH groups in $TiO_2$ coated wool fibers is higher than that of uncoated wool fibers, due to increment in the amount of hydrogen bonded NH groups. As seen in Figure 14, up to around 200°C, the amount of hydrogen bonded NH groups became almost stable for uncoated wool fibers, but that of $TiO_2$ coated wool fibers slightly decreased because some of the water molecules, which had hydrogen bonding with NH groups were removed from the surface of the wool fibers with increasing temperature. After 200°C, a severe decrease in the amount of hydrogen bonded NH groups for both uncoated and $TiO_2$ coated wool were seen. We think that this great decrease is due to a great thermal destruction leading to breakage of intra- and intermolecular interactions such as hydrogen bonds and disulfide crosslinks as well as some covalent bonds in the side chains of amino acids.

## DISCUSSION

The XRF spectra and the SEM images showed that $TiO_2$ coating was formed on the cuticle layer as a network by means of hydrolysis and condensation reactions, which revealed a peak at around 800 $cm^{-1}$ assigned to Ti—O stretching vibrations and changed significantly the absorbance of the bands in the 2700–3700 $cm^{-1}$ region in FTIR/ATR spectrum of $TiO_2$ coated wool fiber. During the formation of $TiO_2$ network on the cuticle layer and hydrolysis and condensation processes, the concentration of H bonded NH groups increased due to hydrogen bond interactions with water molecules appearing. Besides, side chain groups like $CH_3$ and $CH_2$ of some amino acids increased due to the interaction of some remaining residual groups of $TiO_2$ sol. Because $TiO_2$ has affinity toward hydroxyl and carboxylic groups in wool fiber, it has binding with the groups of amino acids such as glutamic acid, aspartic acid, threonine, serine, and tyrosine in the cuticle layer of the wool fiber and has uniform

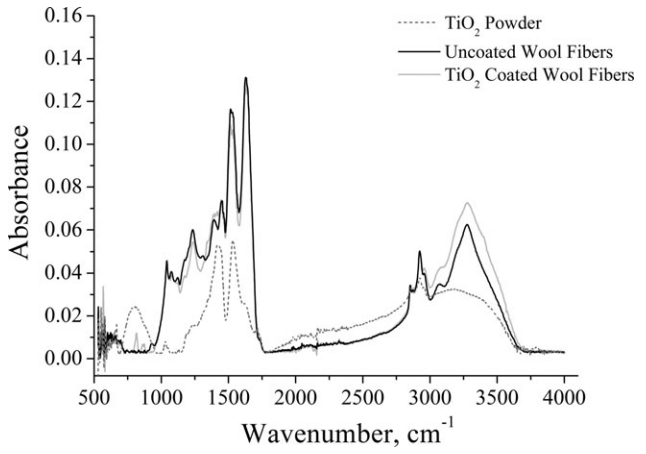


**Figure 9.** The FTIR/ATR spectrum of uncoated, $TiO_2$ coated wool fibers, and $TiO_2$ powder.

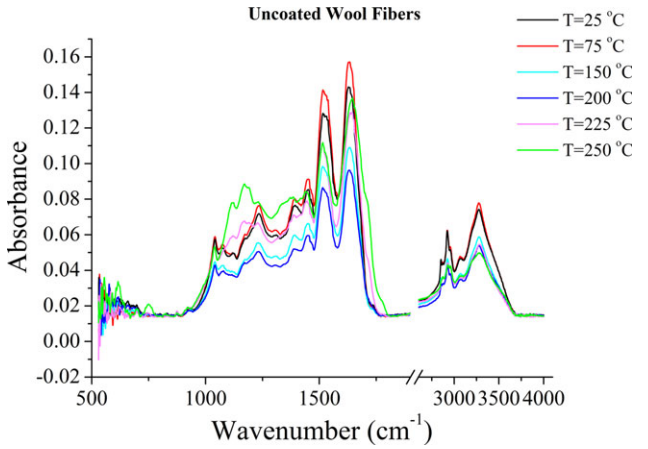


**Figure 10.** The FTIR/ATR spectra of uncoated wool fibers heated at different temperatures. [Color figure can be viewed in the online issue, which is available at wileyonlinelibrary.com.]

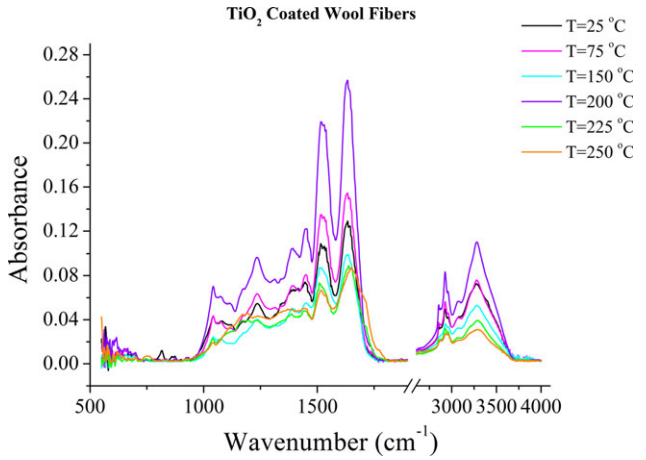


**Figure 11.** The FTIR/ATR spectra of $TiO_2$ coated wool fibers heated at different temperatures. [Color figure can be viewed in the online issue, which is available at wileyonlinelibrary.com.]

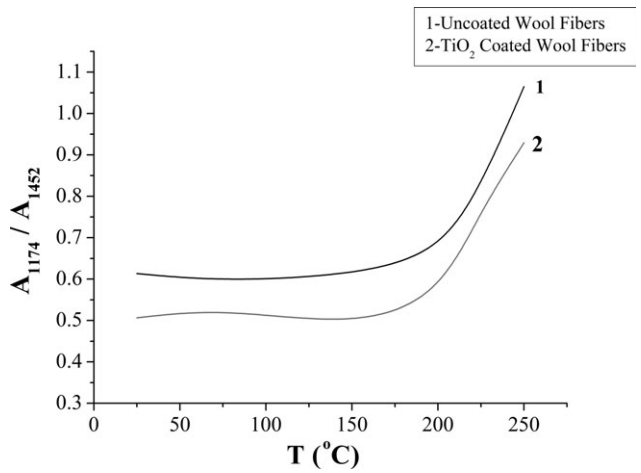


**Figure 13.** The change of the absorbance ratio of asymmetric S=O stretch of sulfonate groups in the wool fibers with increasing thermal treatment temperature.

deposition. Therefore, $TiO_2$ was formed as a network on the cuticle layer and made the surface more rigid and increased the stiffness of the cuticle layer, which has a considerable contribution to the initial or Young's modulus of the fiber. This coating increased significantly the initial modulus of the wool fiber by 19% at room conditions. Although the ultimate tensile stress remained almost unchanged, while the stiffness of the fiber increased, the tensile strain at breaking load decreased slightly. However, the $TiO_2$ coated wool fibers obtained noticeably higher stress levels in three deformation regions up to their rupture point in the stress–strain curves than those for uncoated wool fibers.

In case of thermal treatment, because the thermal treatment up to around 160°C causes the evaporation of water molecules in the fiber structure, especially amorphous matrix of both uncoated and $TiO_2$ coated wool fibers as seen in Figure 8, which led to the changes in the intermolecular hydrogen bond interactions especially between microfibrils and matrix molecules, apparently, the rigidity and the slope of the yield region increased. The uniaxial tensile properties did not deteriorate much. While the initial modulus remained almost constant, the ultimate tensile stress, and breaking extension decreased slightly. The small changes in the tensile properties were also verified by the constancy or small decrease in the absorbance ratios of the bands for N—H stretching of H bonded NH groups, asymmetric C—H stretching of $CH_3$ groups, and asymmetric sulfonate S=O stretching vibrations as we have seen above.

However, the tensile properties especially ultimate tensile stress and breaking extension decreased considerably for both uncoated and $TiO_2$ coated wool fibers after they were exposed to thermal treatment at 200°C and beyond this temperature, that is, the ultimate tensile stress decreased by 27 and 28% for uncoated and $TiO_2$ coated wool fibers and corresponding breaking extension values decreased greatly by about 48 and 64%. Although the initial modulus of the uncoated wool fibers decreased slightly by about 3%, that of $TiO_2$ coated wool fibers decreased by about 15%. As we have seen in the TGA/DSC

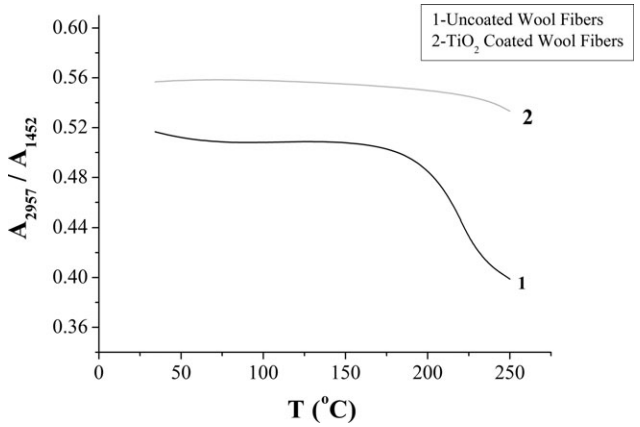


**Figure 12.** The change of absorbance ratio of the asymmetric C—H stretching of $CH_3$ in the wool fibers with increasing thermal treatment temperature.

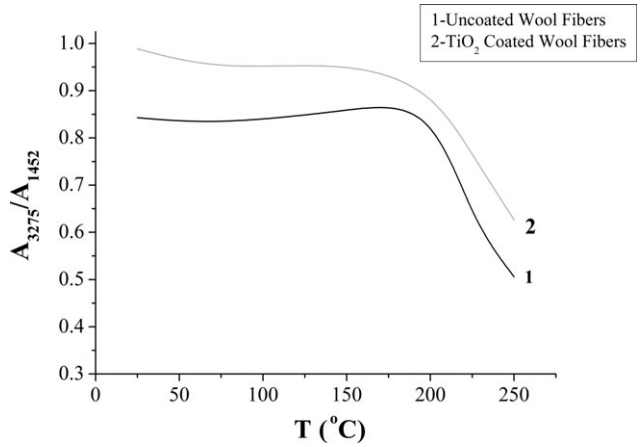


**Figure 14.** The change of absorbance ratio of N—H stretching vibrations of hydrogen bonded NH groups in the wool fibers with increasing thermal treatment temperature.

diagrams, the thermal denaturation of α-helical structure starts at around 200–210°C and a great mass loss, that is, ~41% was observed up to around 360°C. These thermal denaturation and degradation processes led to the rupture of many chemical bonds involved in the cuticle layer and cortex regions including the cleavage of disulfide bonds, which gives a thermal stability to the wool fiber. Therefore, the absorbance ratios of the bands for N—H stretching of H bonded NH groups, asymmetric $CH_3$ groups decreased sharply after around 200°C, and asymmetric S—O stretch of sulfonate groups increased sharply being an evidence of the rupture of disulfide bonds. After thermal treatment at 200°C, the fiber became very brittle and could easily get a powder form, which did not allow us to carry out tensile test. That is, the fibers lost their tensile properties completely after being treated at $T \cong 200$°C.

## CONCLUSIONS

Uniaxial tensile tests revealed that the shape of the stress–strain curve of the $TiO_2$ coated single wool fibers by sol-gel method became the same as that of uncoated wool fibers at room conditions. But, the initial modulus of the $TiO_2$ coated wool fibers, which can be considered as an important characteristic for the stiffness of the wool fibers increased significantly by 19%, which was attributed mostly to the increment in the stiffness of the cuticle layer. It is known that material with a high initial modulus becomes stiffer and harder to deform or deflect under an applied stress than the materials with a low initial modulus. Thus, in addition to benefits of $TiO_2$ coating on the properties of wool fibers such as the improvements in the photostability, antibacterial, antifelting, and self-cleaning properties of the wool fibers, coating a wool fiber with $TiO_2$ by the sol-gel method can be considered as an easily applicable method in order to improve the stiffness of a wool fiber without deteriorating other tensile properties much. It was also observed that while $TiO_2$ coating increased the rigidity of the wool fiber, it decreased the extensibility slightly. The $TiO_2$ coated wool fiber being more rigid than uncoated wool fiber obtained higher yield stress values and stress levels, thereby being stronger in the three deformation regions up to their rupture in the stress–strain curves. The ultimate tensile stress almost became the same as that of uncoated wool fiber and breaking extension decreased slightly by 8%. After the application of heat treatment up to around 160°C, the tensile properties did not deteriorate greatly and both uncoated and $TiO_2$ coated wool fibers showed a similar tensile characteristics. However, by getting a constant value, $TiO_2$ coated wool fiber kept always a higher Young's modulus value than that of uncoated wool fibers. The mass losses of the wool fibers observed in the TGA diagrams were attributed to the evaporation of water molecules from the structure that resulted in the significant changes of the hydrogen bond interactions in the cuticle layer and cortex region.

It was observed that heating from around 200°C up to 360°C in the TGA process caused the denaturation of α-helical structure and following degradation process involving the ruptures of chemical bonds and disulfide crosslinks in both cuticle layer and cortical cells shown with thermal analysis and spectroscopic results. Therefore, the fibers lost the most of the uniaxial tensile properties with a similar tendency after heat treatment at 200°C. That is, the ultimate tensile stress and breaking extension decreased by 27 and 48% for uncoated and by 28 and 64% for $TiO_2$ coated wool fibers, respectively. After heat treatment at around 200°C, the wool fibers became very brittle, which could not allow for conducting tensile tests and lost their tensile properties fully. It is concluded that in addition to improvements in the some properties of wool fibers such as photostability, antibacterial, antifelting, and self-cleaning properties of the wool fibers, which were studied earlier by different researchers, $TiO_2$ coating by sol-gel method increased significantly the initial or Young's modulus at room conditions and kept its constancy even after the wool fibers were exposed to heat treatment up to around 150°C; however, it led to slight decreases in the ultimate tensile stress and extensibility after the wool fibers were heated up to 175°C, after which almost all the uniaxial tensile properties decreased dramatically.

## REFERENCES


1. Feughelman, M. *Text. Res. J.* **1994**, *64*, 236.
2. Feughelman, M. *Text. Res. J.* **1959**, *29*, 223.
3. Feughelman, M. *J. Appl. Polym. Sci.* **2002**, *83*, 489.
4. Liu, H.; Yu, W. *J. Appl. Polym. Sci.* **2007**, *103*, 1.
5. Speakman, J. B.; Hirst, M. C. *Nature* **1931**, *128*, 1073.
6. Church, J. S.; Corino, G. L.; Woodhead, A. L. *Biopolymers* **1997**, *42*, 7.
7. Bradbury, J. H.; Chapman, G. V.; King, N. L. R. *Aust. J. Biol. Sci.* **1965**, *18*, 353.
8. Woods, H. J. *Proc. R. Soc. Lond. A* **1938**, *166*, 76.
9. Lustig, B.; Kondritzer, A. A.; Moore, D. H. *Archiv. Biochem.* **1945**, *8*, 57.
10. Liu, H.; Bryson, W. G. *J. Text. Inst.* **2002**, *93*, 121.
11. Alexandaer, P.; Hudson, R. F.; Earland, C. Wool: Its Chemistry and Physics, 2nd ed.; Chapman & Hall: London, **1963**; p 56, 357.
12. Zhang, H.; Millington, K. R.; Wang, X. *Polym. Degrad. Stab.* **2009**, *94*, 278.
13. Tung, W. S.; Daoud, W. A. *J. Colloid Interface Sci.* **2008**, *326*, 283.
14. Liu, J.; Wang, Q.; Fan, X. R. *J. Sol Gel Sci. Technol.* **2012**, *62*, 338.
15. Hsieh, S. H.; Zhang, F. Ru.; Li, H. S. *J. Appl. Polym. Sci.* **2006**, *100*, 4311.
16. Montazer, M.; Pakdel, E.; Behzadnia, A. *J. Appl. Polym. Sci.* **2011**, *121*, 3407.
17. Montazer, M.; Behzadnia, A.; Moghadam, M. B. *J. Appl. Polym. Sci.* **2012**, *125*, E356.
18. Zhang, H.; Wang, L. L. *J. The Text. Inst.* **2010**, *101*, 842.
19. Tung, W. S.; Daoud, W. A. *Surf. Eng.* **2010**, *26*, 525.
20. Haly, A. R.; Snaith, J. W. *Text. Res. J.* **1970**, *40*, 142.
21. Cao, J.; Joko, K.; Cook, J. R. *Text. Res. J.* **1997**, *67*, 117.
22. Watt, I. C. *Text. Res. J.* **1975**, *45*, 728.

23. Moharram, M. A.; Abdel-Rehim, T. Z.; Rabie, S. M. *J. Appl. Polym. Sci.* **1981**, *26*, 921.
24. Morton, W. E.; Hearle, J. W. S. Physical Properties of Textile Fibres, 4th ed.; Woodhead Publishing: Cambridge, **2008**; p 315.
25. Aksakal, B.; Alekberov, V. *Fibers Polym.* **2009**, *10*, 673.
26. Hinczewski, D. S.; Hinczewski, M.; Tepehan, F. Z.; Tepehan, G. G. *Solar Energy Mater. Sol. Cells* **2005**, *87*, 181.
27. Hearle, J. W. S. *Int. J. Biol. Macromol.* **2000**, *27*, 123.
28. Wortmann, F. J.; Zahn, H. *Text. Res. J.* **1994**, *64*, 737.
29. Chapman, B. M. *Text. Res. J.* **1969**, *39*, 1102.
30. Aksakal, B.; Tsobkallo, K. S.; Darvish, D. *J. Appl. Polym. Sci.*, **2012**, *125*, E168.
31. Xu, W.; Ke, G.; Wu, J.; Wang, X. *Eur. Polym. J.* **2006**, *42*, 2168.
32. Cao, J. *Thermochim. Acta* **1999**, *335*, 5.
33. Tian, C. M.; Li, Z.; Guo, H. Z., Xu, J. Z. *J. Fire Sci.* **2003**, *2*, 155.
34. Davies, P. J.; Horrocks, A. R.; Miraftab, M. *Polym. Int.* **2000**, *49*, 1125.
35. Menefee, E.; Yee, G. *Text. Res. J.* **1965**, *35*, 801.
36. Manich, A. M.; Carilla, J.; Vilchez, S.; de Castellar, M. D.; Oller, P.; Erra, P. *J. Thermal Anal. Calor.* **2005**, *82*, 119.
37. Faria, E. H.; Marçal, A. L.; Nassar, E. J.; Ciuffi, K. J.; Calefi, P. S. *Mater. Res.* **2007**, *10*, 413.
38. Lopez, T.; Sanchez, E.; Bosch, P.; Meas, Y.; Gomez, R. *Mater. Chem. Phys.* **1992**, *32*, 141.
39. Perrin, F. X.; Nguyen, V.; Vernet, J. L. *J. Sol Gel Sci. Tech.* **2003**, *28*, 205.
40. Sui, R.; Thangadurai, V.; Berlinguette, C. P. *Chem. Mater.* **2008**, *20*, 7022.
41. Stuart, B. Modern Infrared Spectroscopy; Wiley: West Sussex, **1996**; p 98, 118.
42. Kuzuhara, A. *Biopolymers* **2005**, *77*, 335.
43. Akhtar, W.; Edwards, H. G. M.; Farwell, D. W.; Nutbrown, M. *Spectrochim. Acta Part A* **1997**, *53*, 1021.
44. Paquin, R.; Colomban, P. *J. Raman Spectrosc.* **2007**, *38*, 504.
45. Weston, G. J. *Biochim Biophys Acta* **1955**, *17*, 462.
46. Strasheim, A.; Buijs, K. *Biochim Biophys Acta* **1961**, *47*, 538.
47. Robbins, C. *Text. Res. J.* **1967**, *37*, 811.
48. Kuzuhara, A. *Biopolymers* **2006**, *85*, 274.
49. Strassburger, J. *J. Soc. Cosmet. Chem.* **1985**, *36*, 61.
50. Wojciechowska, E.; Wlochowicz, A.; Weselucha-Birczynska, A. *J. Molec. Struc.* **1999**, *511–512*, 307.
51. Skrovanek, D. J.; Howe, S. E.; Painter, P. C.; Coleman, M. M. *Macromolecules* **1985**, *18*, 1676.
52. Mayo, D. W.; Miller, F. A.; Hannah, R. W. Course Notes on the Interpretation of Infrared and Raman Spectra; Willey: New Jersey, **2003**; p 48.
53. Tsobkallo, E.; Aksakal, B.; Darvish, D. *J. Macromol. Sci. Part B: Phys.* **2010**, *49*, 495.
54. Daoud, W. A.; Leung, S. K.; Tung, W. S.; Xin, J. H.; Cheuk, K.; Qi, K. *Chem. Mater.* **2008**, *20*, 1242.